

# 具有不同渗透的涨缩管道内微极性流动的同伦分析解\*

司新毅<sup>1</sup>, 司新辉<sup>2</sup>, 郑连存<sup>2</sup>, 张欣欣<sup>3</sup>

- (1. 河海大学 水利水电工程学院,南京 210098;
2. 北京科技大学 数理学院,北京 100083;
3. 北京科技大学 机械学院,北京 100083)

**摘要:** 分析了壁面具有不同渗透的涨缩管道内微极性流体的流动.对于壁面的胀缩,考虑常系数和时间函数的膨胀率两种情况.对于第1种情况,应用同伦分析方法得到该问题的速度和微旋转角度的表达式.并且画图分析了各个不同参数,特别是膨胀系数和不同的渗透率对流体的动力特征的影响.可以得到第1个重要的结论:壁面的膨胀率和不同的渗透率对流体的动力特征有重要的影响.根据 Xu 的模型,考虑了第2种也是更具有一般性的情况,假设壁面的膨胀率随时间的变化而变化.在这样的假设下,控制方程被转化成非线性偏微分方程,并且同样也可以应用 HAM 方法进行求解.应用代数和指数的模型来描述膨胀率从初始状态到最终状态的演变过程.然而,结果表明包含时间的解很快地趋向于稳态的解.这样可以得到第2个重要的结论,时间在壁面的膨胀收缩中扮演着次要的角色,可以忽略不计.

**关键词:** 同伦分析方法; 微极性流体; 涨缩壁面; 多孔管道; 不同渗透速度

**中图分类号:** O175.8;O357.3 **文献标志码:** A

**DOI:** 10.3879/j.issn.1000-0887.2011.07.005

## 引言

在过去的几十年间,圆形或者矩形的渗透壁面的管道内的流动引起了相当的关注.最早的关于静止的渗透壁面的管道流动的工作可以追溯到 Berman<sup>[1]</sup>的工作,控制方程可以转化为一个包含有渗透 Reynolds 数的四阶常微分方程,并且可以得到相应的解.自此以后,做了大量的关于对称的静止壁面的工作<sup>[2-6]</sup>.特别是 Terrill<sup>[6]</sup>对非对称渗透的两平行平板间的层流进行了分析.

由于在脉动隔膜模型、过滤、血液流动和人工透析,同位素分离、呼吸系统的气体 and 血液循环模型等生物物理领域的广泛应用,可膨胀或收缩的多孔管道流动也引起了科研工作者的

\* 收稿日期: 2010-12-06; 修订日期: 2011-04-20

**基金项目:** 国家自然科学基金资助项目(50936003;50905013);先进金属和材料国家重点实验室项目(2009Z-02)

**作者简介:** 司新毅(1985—),男,山东聊城人,博士生(E-mail:hotsauce0079@163.com);  
司新辉(1978—),男,山东聊城人,讲师,博士(联系人.Tel:+86-10-62332589;  
E-mail:sixinhui\_ustb@126.com).

注意,特别是生物组织内的管道流动常常被认为是在一个胀缩渗透管道的流体流动.例如,带有阀门的管道具有可变形的边界,由于边界的交替收缩产生生物泵的特征.而且,肾脏中的流动也体现了相似的行为特征<sup>[7]</sup>. Uchida 等<sup>[8]</sup>首先对壁面可径向收缩、不可渗透管道内不可压缩流体的非稳态流动进行了研究. Ohki<sup>[9]</sup>讨论了考虑壁面吸附喷注情况下,半无限长、轴向随时间变化而径向不变的圆形管道中流体流动.为了模拟固体发动机内的层流流动, Goto 等<sup>[10]</sup>分析了壁面随时间径向变化半无限长圆管的不可压缩流体的层流流动. Bujurke 等<sup>[11]</sup>得到了胀缩圆形管道中非稳态流动的级数解. Majdalani, Zhou 和 Dauenhauer 等<sup>[12-14]</sup>得到不同 Reynolds 数下的数值解和渐近解. Asghar 等<sup>[15]</sup>应用 AMD 方法讨论了弱渗透情况下的缓慢变形管道内的流动. Si 等的文献<sup>[16]</sup>得到非对称的 Newton 流在胀缩渗透管道中流动的解析解,并且讨论了微极性流体在胀缩管道中的流动情况<sup>[17-18]</sup>. 然而以上所有的工作,均考虑壁面的膨胀系数为一常数.为了讨论该模型的更一般的情况, Xu 等<sup>[19]</sup>对 Dauenhauer-Majdalani 模型进行了推广,认为壁面的膨胀率不再是一个常数,而是一个和时间相关的变量,其变化的范围从  $\alpha_0$  到  $\alpha_1$ , 这样, Dauenhauer-Majdalani 的模型是 Xu 的一种特殊情况. 最近, Makukula<sup>[20]</sup>应用谱同伦的方法重新讨论了该问题,而且 Si 等人把该问题推广到粘弹性流体<sup>[21]</sup>.

事实上,工业和科技中很多重要的流体都体现出非 Newton 流的特征. Eringen<sup>[22-23]</sup>首先提出了微极性流体的理论并且推导出微结构流体的本构定律. 该理论为一些具有非 Newton 行为的流体,像聚合物、胶状悬浮液、动物血液、液晶等,提供了数学模型. 关于微极性流体的综述性的论述可以参考文献<sup>[24-26]</sup>. 而且 Subhadra 等<sup>[27]</sup>、Takhar 等<sup>[28]</sup>、Kelson 和 Farrell<sup>[29]</sup>、Muhammad Ashraf, Anwar Kamal, Syed<sup>[30-31]</sup>等多人都数值计算了吸附或喷注管道内的微极性流动.

基于上述的工作,本文对具有不同渗透胀缩边界的管道内的微极性流动进行了分析. 应用 Liao<sup>[32-33]</sup>提出的同伦分析方法(HAM),计算该问题的速度场. 而且 Hayat 等<sup>[34-36]</sup>、Abbas 等<sup>[37]</sup>和 Sajid 等<sup>[38-39]</sup>已经应用同伦分析方法成功地解决了一些非线性问题. 本文讨论了不同的参数,特别是膨胀率,对速度场和微旋转角速度的影响并且以图形的形式表示,进行分析.

## 1 问题模型

我们考虑一半无限长可渗透胀缩管道中的非稳态微极性流体. 两壁面之间的距离为  $2a(t)$ , 远小于其宽度和长度. 管道的一端被复杂的固体薄膜所封闭. 两壁面具有不同的渗透

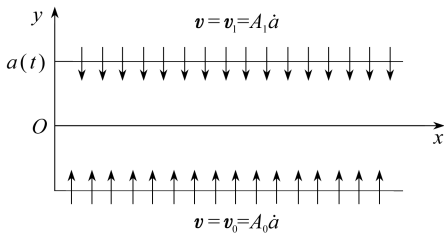


图1 胀缩渗透管道流动模型

Fig. 1 The model of the porous channel with expanding or contracting walls

速度  $v_0, v_1$ , 且以相同的速率  $\dot{a}(t)$  膨胀或者收缩. 如图1所示,建立坐标系,  $x, y$  轴分别平行、垂直于管道中心.  $u, v$  和  $N$  分别表示  $x, y$  方向的速度分量,微旋转角速度.

如以上假设,控制方程表述如下<sup>[40]</sup>:

$$\frac{\partial u}{\partial x} + \frac{\partial v}{\partial y} = 0, \quad (1)$$

$$\begin{aligned} \frac{\partial u}{\partial t} + u \frac{\partial u}{\partial x} + v \frac{\partial u}{\partial y} = -\frac{1}{\rho} \frac{\partial p}{\partial x} + \\ \left( \nu + \frac{\kappa}{\rho} \right) \left( \frac{\partial^2 u}{\partial x^2} + \frac{\partial^2 u}{\partial y^2} \right) + \frac{\kappa}{\rho} \frac{\partial N}{\partial y}, \end{aligned} \quad (2)$$

$$\frac{\partial v}{\partial t} + u \frac{\partial v}{\partial x} + v \frac{\partial v}{\partial y} = -\frac{1}{\rho} \frac{\partial p}{\partial y} + \left( \nu + \frac{\kappa}{\rho} \right) \left( \frac{\partial^2 v}{\partial x^2} + \frac{\partial^2 v}{\partial y^2} \right) - \frac{\kappa}{\rho} \frac{\partial N}{\partial x}, \quad (3)$$

$$\rho j \left( \frac{\partial N}{\partial t} + u \frac{\partial N}{\partial x} + v \frac{\partial N}{\partial y} \right) = -\kappa \left( 2N + \frac{\partial u}{\partial y} - \frac{\partial v}{\partial x} \right) + \gamma \left( \frac{\partial^2 N}{\partial y^2} + \frac{\partial^2 N}{\partial x^2} \right), \quad (4)$$

这里,  $\rho, \nu$  为密度, 粘性系数,  $j, \gamma, \kappa$  分别表示单位质量的微惯性, 旋转梯度粘度, 涡流粘度系数. 这里  $\gamma$  可以表示为<sup>[41]</sup>

$$\gamma = \left( \mu + \frac{\kappa}{2} \right) j, \quad (5)$$

这里  $\mu$  为动力粘性系数. 由于微元素在壁面附近的强聚集性, 我们假设靠近壁面的微元素处于静止状态, 没有旋转<sup>[42]</sup>. 以  $j = a^2$  作为参考长度, 则相应的边界条件为<sup>[5-6, 16-17]</sup>:

$$u(x, -a) = 0, \quad v(x, -a) = v_0 = A_0 \dot{a}, \quad N(x, -a) = 0, \quad u(0, y) = 0, \quad (6)$$

$$u(x, a) = 0, \quad v(x, a) = v_1 = A_1 \dot{a}, \quad N(x, a) = 0, \quad (7)$$

这里,  $A_0 = v_0/\dot{a}$ ,  $A_1 = v_1/\dot{a}$  为喷注系数, 用来表征壁面的渗透强度.

定义

$$u = -\nu a^{-2} x F_\eta(\eta, t), \quad v = \nu a^{-1} F(\eta, t), \quad N = \nu a^{-3} x G(\eta, t), \quad \eta = \frac{y}{a(t)}. \quad (8)$$

把式(8)代入式(1)~(4), 可以得到微分方程组:

$$(1 + K) F_{\eta\eta\eta} - K G_{\eta\eta} + 3\alpha F_{\eta\eta} + \alpha \eta F_{\eta\eta\eta} + (F_\eta F_{\eta\eta} - F F_{\eta\eta\eta}) - \nu^{-1} a^2 F_{\eta\eta t} = 0, \quad (9)$$

$$\left( 1 + \frac{K}{2} \right) G_{\eta\eta} + 3\alpha G + \alpha \eta G_\eta + (F_\eta G - F G_\eta) - K(2G - F_{\eta\eta}) - \nu^{-1} a^2 G_t = 0, \quad (10)$$

这里,  $K = \kappa/\mu$ .  $\alpha$  为壁面膨胀率, 定义为  $\alpha = a\dot{a}/\nu$ . 当壁面膨胀时, 膨胀率为正数, 收缩时为负数.

边界条件为

$$F_\eta = 0, \quad F = Re_1 = A_0 \alpha, \quad G = 0, \quad \eta = -1, \quad (11)$$

$$F_\eta = 0, \quad F = Re = A_1 \alpha, \quad G = 0, \quad \eta = 1, \quad (12)$$

这里,  $Re, Re_1$  为渗透 Reynolds 数, 分别表示为  $Re = av_0/\nu, Re_1 = av_1/\nu$ . 从物理意义上讲, 其值为正时, 表示吸附, 为负时表示喷注.

### 1.1 定壁面膨胀率的相似方程

引入 Uchida 和 Aoki<sup>[8]</sup>、Majdalani 等<sup>[12]</sup>、Dauenhauer 和 Majdalani<sup>[13]</sup> 分别所提出的时间和空间上的相似变换, 即假设  $\alpha$  为常数并且  $f = f(\eta)$ , 这样  $f_{\eta\eta t} = 0$ . 相似地, 我们假设  $g = g(\eta)$ . 从物理的角度来看<sup>[8, 12-14]</sup>, 基于下述假设, 该模型认为壁面运动速度随着半径的增大而减少,

$$\alpha = \frac{\dot{a}a}{\nu} = \frac{\dot{a}_0 a_0}{\nu} = \text{const}, \quad (13)$$

这里,  $a_0$  和  $\dot{a}_0$  分别表示初始的管道高度和膨胀速度. 对式(13)进行积分, 即可得到相似解. 其结果为

$$\frac{a}{a_0} = \frac{v_w(0)}{v_w(t)} = \sqrt{1 + 2\nu\alpha t a_0^{-2}}. \quad (14)$$

因为  $v_i = A_i \dot{a}$ ,  $A_i = \text{const}$ <sup>[10, 13]</sup>, 则可以得到壁面的喷注速度的表达式.

令

$$f = \frac{F}{Re}, \quad g = \frac{G}{Re}, \quad (15)$$

根据上述假设,微分方程组可以变为

$$(1 + K)f^{(4)} - Kg'' + 3\alpha f'' + \alpha\eta f''' + Re(f'f'' - ff''') = 0, \quad (16)$$

$$\left(1 + \frac{K}{2}\right)g'' + 3\alpha g + \alpha\eta g' + Re(f'g - fg') - K(2g - f'') = 0. \quad (17)$$

边界条件为

$$f'(\eta) = 0, f(\eta) = A, g(\eta) = 0, \eta = -1, \quad (18)$$

$$f'(\eta) = 0, f(\eta) = 1, g(\eta) = 0, \eta = 1, \quad (19)$$

这里  $A = Re_1/Re = v_0/v_1$ . 当  $\alpha = 0, A = -1$  时,这就是 Takhar 等<sup>[28]</sup>曾讨论过的情况.

## 1.2 非定常系数壁面膨胀率的流动方程

实际上,壁面的膨胀率  $\alpha(t)$  严格来讲并不是一个常数,而是时间  $t$  的函数,从  $\alpha_0$  变化到  $\alpha_1$ . 假设

$$\beta(t) = \frac{a^2}{\nu}, \quad (20)$$

$$\text{则 } \alpha(t) = \frac{a\dot{a}}{\nu} = \frac{1}{2}\beta_t(t), \quad (21)$$

$$\alpha_0(t) = \alpha(0) = \frac{a_0\dot{a}_0}{\nu} = \frac{1}{2}\beta_t(0). \quad (22)$$

根据如上的假设,  $A_i (i = 0, 1)$  与  $\alpha(t)$  成反比,则方程(9)和(10)表示成

$$(1 + K)F_{\eta\eta\eta\eta} - KG_{\eta\eta} + 3\alpha(t)F_{\eta\eta} + \alpha(t)\eta F_{\eta\eta\eta} + (F_{\eta}F_{\eta\eta} - FF_{\eta\eta\eta}) - \beta(t)F_{\eta\eta} = 0, \quad (23)$$

$$\left(1 + \frac{K}{2}\right)G_{\eta\eta} + 3\alpha(t)G + \alpha(t)\eta G_{\eta} + (F_{\eta}G - FG_{\eta}) - K(2G - F_{\eta\eta}) - \beta(t)G_t = 0. \quad (24)$$

相应的边界条件为

$$F_{\eta}(\eta, t) = 0, F(\eta, t) = Re_1, G(\eta, t) = 0, \eta = -1, \quad (25)$$

$$F_{\eta}(\eta, t) = 0, F(\eta, t) = Re, G(\eta, t) = 0, \eta = 1. \quad (26)$$

## 2 定膨胀率下速度和角速度的同伦分析解

这里我们选择初始函数

$$f_0(\eta) = \frac{A-1}{4}\eta^3 + \frac{3-3A}{4}\eta + \frac{A+1}{2}, g_0(\eta) = 0 \quad (27)$$

和辅助线性算子

$$\mathcal{L}_1(f) = f^{(4)}, \mathcal{L}_2(g) = g''. \quad (28)$$

辅助算子满足

$$\mathcal{L}_1(C_1 + C_2\eta + C_3\eta^2 + C_4\eta^3) = 0, \mathcal{L}_2(C_5 + C_6\eta) = 0, \quad (29)$$

这里  $C_i (i = 1 \sim 6)$  为任意常数.

由以上定义,可得零阶形变方程

$$(1-p)\mathcal{L}_1(\hat{f} - f_0) = ph\mathfrak{N}_1(\hat{f}, \hat{g}), \quad (30)$$

$$\hat{f}'(-1, p) = 0, \hat{f}(-1, p) = A, \hat{f}'(1, p) = 0, \hat{f}(1, p) = 1, \quad (31)$$

$$(1-p)\mathcal{L}_2(\hat{g} - g_0) = ph\mathfrak{N}_2(\hat{f}, \hat{g}), \quad (32)$$

$$\hat{g}'(-1, p) = 0, \hat{g}(1, p) = 0, \quad (33)$$

$$\begin{aligned} \aleph_1(\hat{f}, \hat{g}) = & (1 + K) \frac{\partial^4 \hat{f}(\eta, p)}{\partial \eta^4} + Re \left( \frac{\partial \hat{f}(\eta, p)}{\partial \eta} \frac{\partial^2 \hat{f}(\eta, p)}{\partial \eta^2} - \hat{f}(\eta, p) \frac{\partial^3 \hat{f}(\eta, p)}{\partial \eta^3} \right) + \\ & 3\alpha \frac{\partial^2 \hat{f}(\eta, p)}{\partial \eta^2} + \alpha \eta \frac{\partial^3 \hat{f}(\eta, p)}{\partial \eta^3} - K \frac{\partial^2 \hat{g}(\eta, p)}{\partial \eta^2}, \end{aligned} \quad (34)$$

$$\begin{aligned} \aleph_2(\hat{f}, \hat{g}) = & \left( 1 + \frac{K}{2} \right) \frac{\partial^2 \hat{g}(\eta, p)}{\partial \eta^2} + Re \left( \frac{\partial \hat{f}(\eta, p)}{\partial \eta} \hat{g}(\eta, p) - \hat{f}(\eta, p) \frac{\partial \hat{g}(\eta, p)}{\partial \eta} \right) + \\ & 3\alpha \hat{g}(\eta, p) + \alpha \eta \frac{\partial \hat{g}(\eta, p)}{\partial \eta} - K \left( 2\hat{g}(\eta, p) - \frac{\partial^2 \hat{f}(\eta, p)}{\partial \eta^2} \right), \end{aligned} \quad (35)$$

这里,  $p \in [0, 1]$  为嵌入变量,  $h$  为非零辅助参数. 当  $p$  由 0 连续变到 1,  $\hat{f}(\eta, p), \hat{g}(\eta, p)$  分别由初始函数  $f_0(\eta), g_0(\eta)$  变成  $f(\eta), g(\eta)$ . 应用 Taylor 定理, 可得

$$\hat{f}(\eta, p) = f_0(\eta) + \sum_{m=1}^{\infty} f_m(\eta) p^m, \quad f_m(\eta) = \frac{1}{m!} \left. \frac{\partial^m \hat{f}(\eta, p)}{\partial p^m} \right|_{p=0}, \quad (36)$$

$$\hat{g}(\eta, p) = g_0(\eta) + \sum_{m=1}^{\infty} g_m(\eta) p^m, \quad g_m(\eta) = \frac{1}{m!} \left. \frac{\partial^m \hat{g}(\eta, p)}{\partial p^m} \right|_{p=0}, \quad (37)$$

这两个级数的收敛性强烈依靠于  $h$ . 一旦选定了合适的  $h$ , 级数(36)和(37)在  $p=1$  收敛. 由级数(36)和(37)可得

$$f = f_0(\eta) + \sum_{m=1}^{\infty} f_m(\eta), \quad (38)$$

$$g = g_0(\eta) + \sum_{m=1}^{\infty} g_m(\eta). \quad (39)$$

对方程(30)和(32)关于  $p$  求  $m$  次导数, 然后令  $p=0$ , 除以  $m!$ , 可以得到  $m$  阶形变方程:

$$\mathcal{L}_1(f_m(\eta) - \chi_m f_{m-1}(\eta)) = h \aleph_m^f(\eta), \quad (40)$$

$$f'_m(-1) = 0, f_m(-1) = 0, f'_m(1) = 0, f_m(1) = 0, \quad (41)$$

$$\begin{aligned} \aleph_m^f(\eta) = & (1 + K) f_{m-1}^{(4)} + 3\alpha f_{m-1}'' + \alpha \eta f_{m-1}''' - K g_{m-1}'' + \\ & \sum_{k=0}^{m-1} Re(f'_{m-k-1} f_k'' - f_{m-k-1} f_k'''), \end{aligned} \quad (42)$$

$$\mathcal{L}_2(g_m(\eta) - \chi_m g_{m-1}(\eta)) = h \aleph_m^g(\eta), \quad (43)$$

$$g_m(-1) = 0, g_m(1) = 0, \quad (44)$$

$$\begin{aligned} \aleph_m^g(\eta) = & \left( 1 + \frac{K}{2} \right) g_{m-1}'' + 3\alpha g_{m-1} + \alpha \eta g_{m-1}' - K(2g_{m-1} - f_{m-1}') + \\ & \sum_{k=0}^{m-1} Re(f'_{m-k-1} g_k - f_{m-k-1} g_k'), \end{aligned} \quad (45)$$

这里

$$\chi_m = \begin{cases} 0, & m \leq 1, \\ 1, & m > 1. \end{cases} \quad (46)$$

方程(40)和(43)的通解为

$$f_m(\eta) = f_m^*(\eta) + C_1 + C_2 \eta + C_3 \eta^2 + C_4 \eta^3, \quad (47)$$

$$g_m(\eta) = g_m^*(\eta) + C_5 + C_6 \eta, \quad (48)$$

这里,  $f_m^*(\eta), g_m^*(\eta)$  表示方程(40)和(43)的特解, 利用边界条件(41)和(44), 可以确定积分常数  $C_i (i = 1 \sim 6)$ . 应用 Maple, 可以很容易地对方程(40)和(43)逐次求解.

### 3 结果讨论

如 Liao<sup>[43]</sup>所指出,级数(29)和(30)的收敛性依赖于  $h$ .  $h$  的值确定了 HAM 的收敛区间和收敛速度.从理论上对于  $m$  阶近似值可以定义平方残差公式,通过图 2 确定非零辅助参数  $h$ .

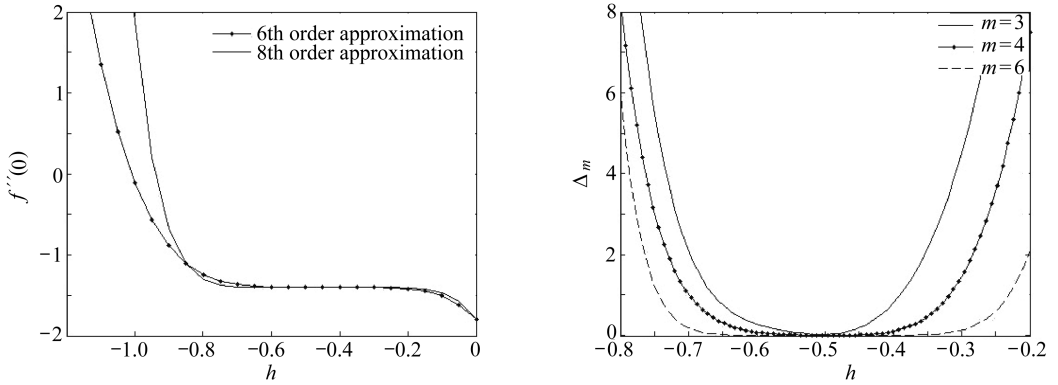


图 2 当  $\alpha = -1, K = 1, Re = 3, A = -0.2$  时,关于  $f''(0)$  的  $h$  曲线以及残差  $\Delta_m$  的变化曲线

Fig. 2  $h$ - curves of  $f''(0)$  and the exact residual error  $\Delta_m$  when  $\alpha = -1, K = 1, Re = 3, A = -0.2$

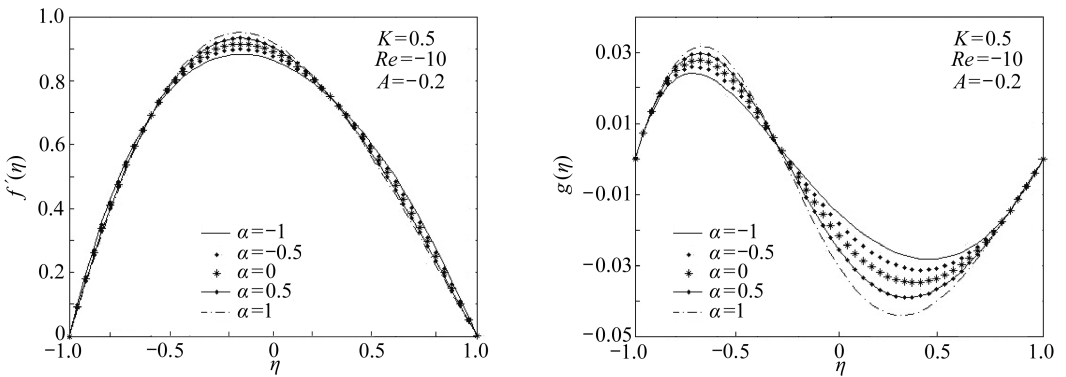


图 3 当  $Re = -10, K = 0.5, A = -0.2$  时,不同的  $\alpha$  影响下  $f', g$  的变化曲线

Fig. 3 Characteristics of  $f', g$  for different  $\alpha$  as  $Re = -10, K = 0.5, A = -0.2$

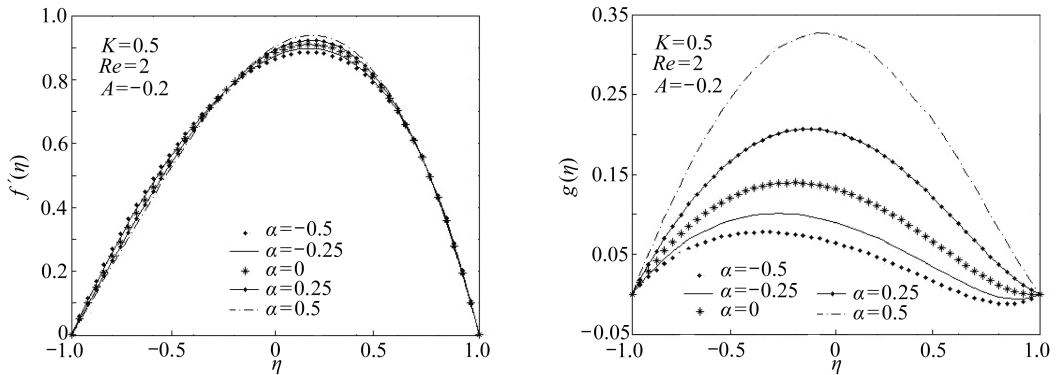


图 4 当  $K = 0.5, Re = 2, A = -0.2$  时,不同的  $\alpha$  影响下  $f', g$  的变化曲线

Fig. 4 Characteristics of  $f', g$  for different  $\alpha$  as  $K = 0.5, Re = 2, A = -0.2$

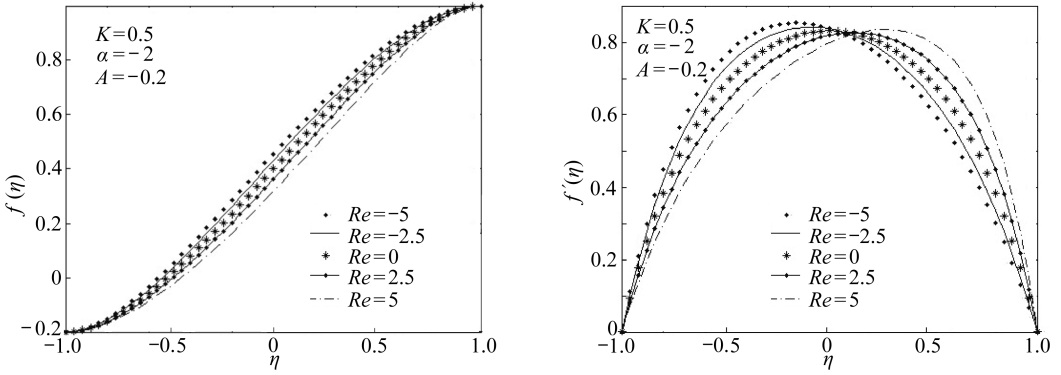


图5 当  $\alpha = -2, K = 0.5, A = -0.2$  时,不同的  $Re$  影响下  $f, f'$  的变化曲线

Fig.5 Characteristics of  $f, f'$  for different  $Re$  as  $\alpha = -2, K = 0.5, A = -0.2$

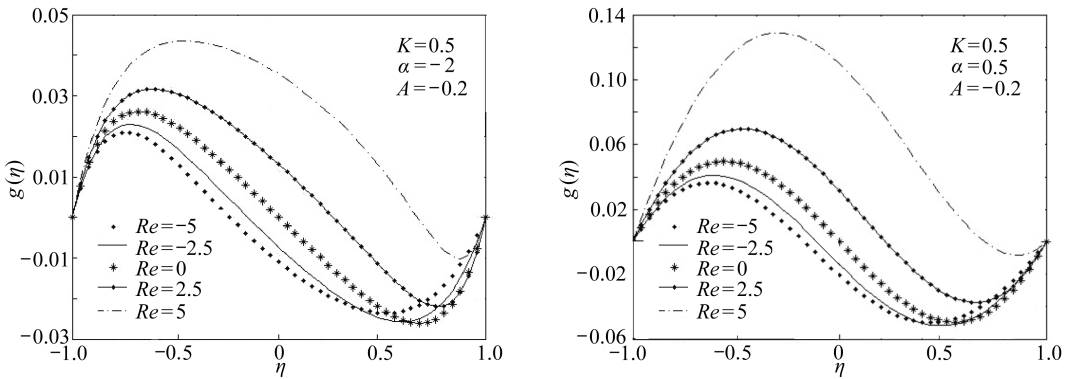


图6 当  $A = -0.2, K = 0.5$  时,不同的  $Re$  影响下  $g$  的变化曲线

Fig.6 Characteristics of  $g$  for different  $Re$  as  $A = -0.2, K = 0.5$

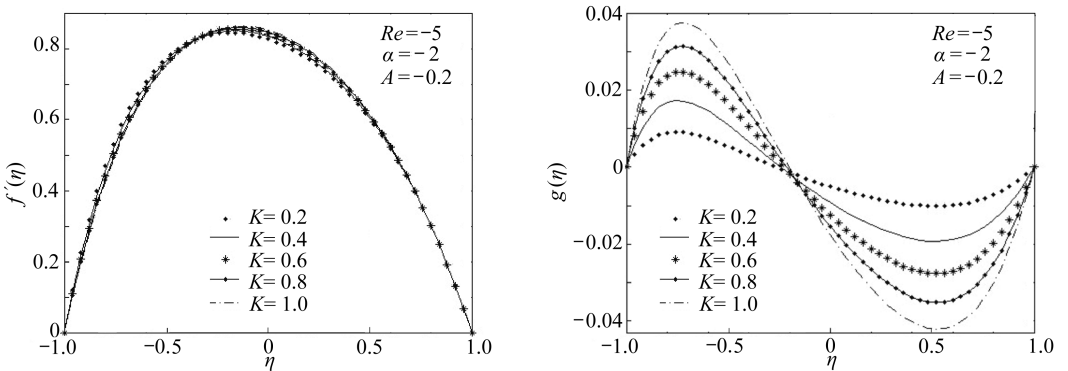


图7 当  $\alpha = -2, Re = -5, A = -0.2$  时,不同的  $K$  影响下  $f', g$  的变化曲线

Fig.7 Characteristics of  $f', g$  for different  $K$  as  $\alpha = -2, Re = -5, A = -0.2$

$$\Delta_m = \int_{-1}^1 \left[ \aleph_1 \left( \sum_{n=1}^m f_n(\eta) \right) \right]^2 + \left[ \aleph_2 \left( \sum_{n=1}^m g_n(\eta) \right) \right]^2 d\eta. \quad (49)$$

图3和图4给出了 $\alpha$ 对 $f'(\eta), g(\eta)$ 的影响曲线.当 $\alpha = 0$ 时,这意味着壁面处于静止状态,若 $A = -0.2$ ,速度图像是非对称的并且速度的最大值介于管道的中心和壁面之间.而且,当壁面膨胀的时候,速度的最大值变大;当壁面收缩的情况下,最大值减小.作为一般的变化趋

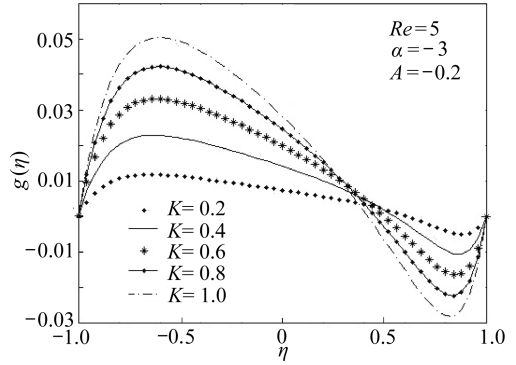
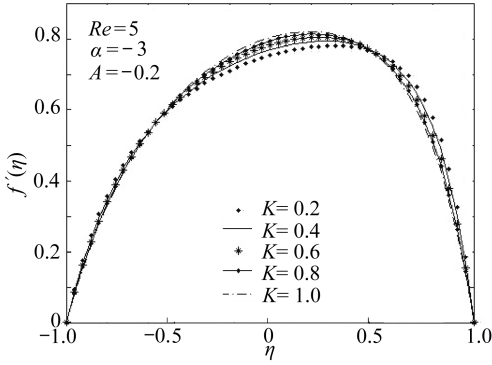


图 8 当  $\alpha = -3, Re = 5, A = -0.2$  时,不同的  $K$  影响下  $f', g$  的变化曲线

Fig. 8 Characteristics of  $f', g$  for different  $K$  as  $\alpha = -3, Re = 5, A = -0.2$

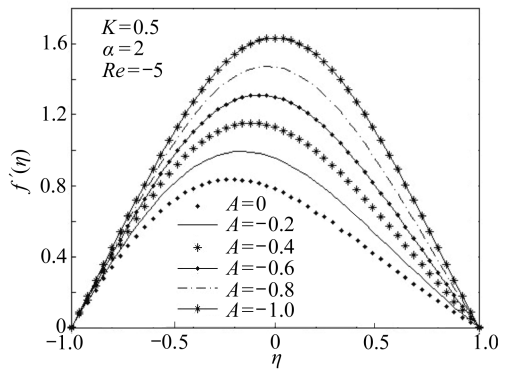
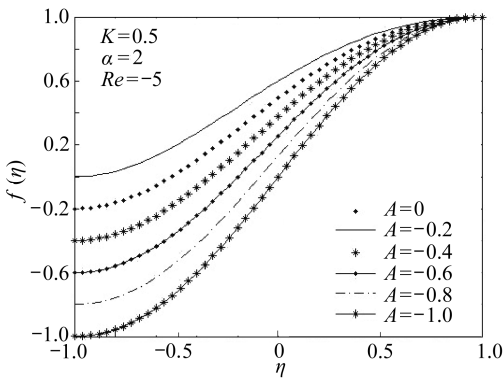


图 9 当  $\alpha = 2, K = 0.5, Re = -5$  时,不同的  $A$  影响下  $f, f'$  的变化曲线

Fig. 9 Characteristics of  $f, f'$  for different  $A$  as  $\alpha = 2, K = 0.5, Re = -5$

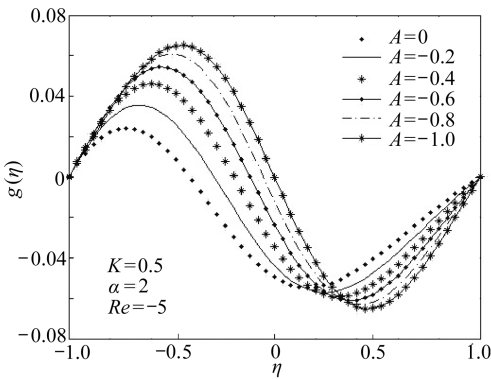


图 10 当  $\alpha = 2, K = 0.5, Re = -5$  时,不同的  $A$  影响下  $g$  的变化曲线

Fig. 10 Characteristics of  $g$  for different  $A$  as  $\alpha = 2, K = 0.5, Re = -5$

势,当  $Re = -10$  时,无论壁面的膨胀系数  $\alpha$  如何变化,微旋转速度改变其凹凸性.然而,当  $Re = 2$  时,随着  $\alpha$  的增加,极值点逐渐消失并且  $g(\eta)$  是  $\alpha$  的增函数.

图 5 和图 6 描述了当壁面收缩的情况下, Reynolds 数  $Re$  对速度和微旋转速度的影响.  $f$  是  $Re$  的减函数.无论  $Re$  如何取值,  $f'$  是非对称的,且最大值介于管道中心和壁面之间.由图 6 中可以看出,在壁面附近微旋转速度具有相反的符号,在两壁面之间有一个零点和两个极值点.相反的符号说明在壁面上剪切应力以相反的方向作用于流体,微极性速度的零点说明这时相反方向的旋转处于平衡的状态.当壁面膨胀时,其图形有相似的变化趋势.

图 7 和图 8 给出了速度和微旋转速度随系数  $K$  的变化曲线.速度的最大值随  $K$  的增大而增大.对于微旋转速度,在靠近壁面附近,有两个极值点和一个零点.当  $Re = 5$  时,零点介于管道中心和上壁面之间,当  $Re = -5$  时,零点介于管道中心和下壁面之间.

图 9 和图 10 给出了两壁面喷注速度的比值  $A$  对  $f, f', g$  的影响.  $f$  为  $A$  的增函数, 而  $f'$  随着  $A$  的减小而增大, 而且其图像变得更加的对称.

### 4 非定常膨胀率下速度和角速度的同伦分析解

以上的工作着重分析当壁面的膨胀率为常数, 速度和微旋转速度在参数的影响下的变化情况. 在下面的工作中, 我们考虑壁面的膨胀率是时间的变量. 沿用 Xu 等的文献[19]中模型的假设, 令

$$\alpha(t) = \alpha_0 \exp(-t) + \alpha_1 [1 - \exp(-t)] \tag{50}$$

和

$$\alpha(t) = \alpha_0 + (\alpha_1 - \alpha_0) \frac{t}{1+t}, \tag{51}$$

其都满足条件

$$\alpha(0) = \alpha_0, \lim_{t \rightarrow +\infty} \alpha(t) = \alpha_1. \tag{52}$$

可以得到  $\beta(t)$  分别为

$$\beta(t) = -2\alpha_0 \exp(-t) + 2\alpha_1 t + 2\alpha_1 \exp(-t) \tag{53}$$

和

$$\beta(t) = 2\alpha_1 t + 2(\alpha_0 - \alpha_1) \ln(1+t). \tag{54}$$

这样, 方程(23)和(24)及其边界条件(25)和(26)可以通过 HAM 来求解.  $F(\eta, t), G(\eta, t)$  的级数表达式为

$$F(\eta, t) = F_0(\eta, t) + \sum_{m=1}^{\infty} F_m(\eta, t), \tag{55}$$

$$G(\eta, t) = G_0(\eta, t) + \sum_{m=1}^{\infty} G_m(\eta, t), \tag{56}$$

这里,  $F(\eta, t), G(\eta, t)$  可以由高阶形变公式确定.

$$\mathcal{L}_1 (F_m(\eta, t) - \chi_m F_{m-1}(\eta, t)) = h \phi_m^F(\eta, t), \tag{57}$$

$$\mathcal{L}_2 (G_m(\eta, t) - \chi_m G_{m-1}(\eta, t)) = h \phi_m^G(\eta, t), \tag{58}$$

相应的边界条件为

$$F_{m\eta}(\eta, t) = 0, F_m(\eta, t) = 0, G_m(\eta, t) = 0, \eta = -1 \tag{59}$$

$$F_{m\eta}(\eta, t) = 0, F_m(\eta, t) = 0, G_m(\eta, t) = 0, \eta = 1, \tag{60}$$

这里

$$\begin{aligned} \phi_m^F(\eta, t) = & (1 + K) F_{m-1}^{(4)} + 3\alpha(t) F_{m-1}'' + \alpha(t) \eta F_{m-1}''' - K G_{m-1}'' + \\ & \sum_{k=0}^{m-1} (F'_{m-k-1} F''_k - F_{m-k-1} F'''_k) - \beta(t) \dot{S}', \end{aligned} \tag{61}$$

$$\begin{aligned} \phi_m^G(\eta, t) = & \left(1 + \frac{K}{2}\right) G_{m-1}'' + 3\alpha(t) G_{m-1} + \alpha(t) \eta G'_{m-1} - K(2G_{m-1} - F''_{m-1}) + \\ & \sum_{k=0}^{m-1} (F'_{m-k-1} G_k - F_{m-k-1} G'_k) - \beta(t) \dot{E}, \end{aligned} \tag{62}$$

这里, “'”和“·”分别表示对  $\eta$  和  $t$  求偏导数. 辅助线性算子  $\mathcal{L}_1, \mathcal{L}_2$  同式(28)和(29)一致,  $\chi_m$  与式(46)一样. 相似地, 选择初始函数

$$F_0(\eta, t) = \frac{2 - 3\eta + \eta^3}{4} Re_1 + \frac{2 + 3\eta - \eta^3}{4} Re, g_0(\eta, t) = 0, \tag{63}$$

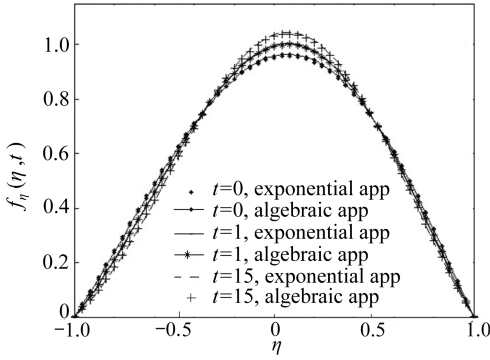


图 11 当  $\alpha_0 = 1, \alpha_1 = 2, Re_1 = 1, Re = -0.2$  时,  $F_\eta(\eta, t)$  随时间的变化曲线

Fig. 11 The comparison of  $F_\eta(\eta, t)$  for different time as  $\alpha_0 = 1, \alpha_1 = 2, Re_1 = 1, Re = -0.2$

则原来的偏微分方程组 (57) 和 (58) 可以应用 HAM 转化成一系列线性常微分方程组来进行计算。

对于固定的参数  $Re = 1, Re_1 = -0.2, K = 0.1$ , 当  $\alpha(t)$  从 1 变化到 2 时, 图 11, 12, 13 描述了其解对时间的敏感性. 图 11 显示了对于指数和代数形式的膨胀率情况下两族曲线的一致性. 由图 12 可以看出, 当时间大于 5 时, 两族曲线之间的差别几乎不可见。

图 13 描述了当  $\alpha(t)$  从 1 变化到 2 和从 2 变化到 1 时,  $F_\eta(0, t), G_\eta(0, t)$  随时间的变化曲线. 当时间超过 5 时,  $F_\eta(0, t), G_\eta(0, t)$  平行于  $x$  轴. 这说明速度会很快地趋向于稳定的状态. 这样从另外的角度帮我们确认了前面假设的可靠性: 时间的变化是可以忽略的, 原来的控制方程可以转化为常微分方程组。

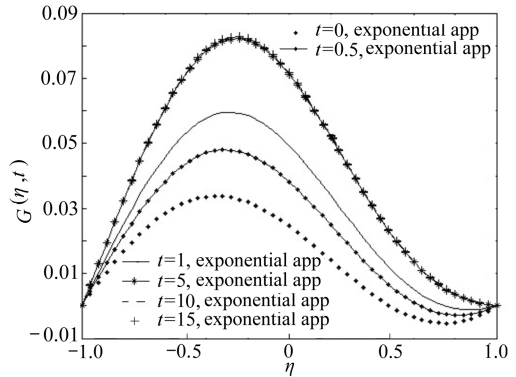
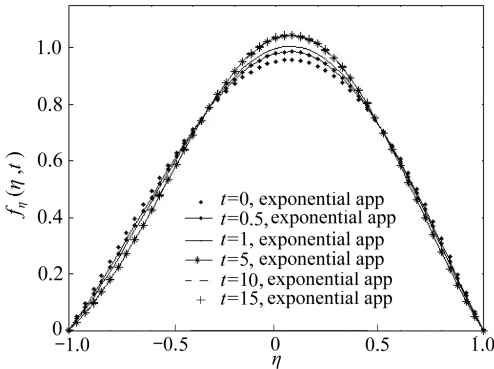


图 12 当  $\alpha_0 = 1, \alpha_1 = 2, Re_1 = 1, Re = -0.2$  时,  $F_\eta(\eta, t), G(\eta, t)$  随时间的变化曲线

Fig. 12 The comparison of  $F_\eta(\eta, t), G(\eta, t)$  for different time as  $\alpha_0 = 1, \alpha_1 = 2, Re_1 = 1, Re = -0.2$

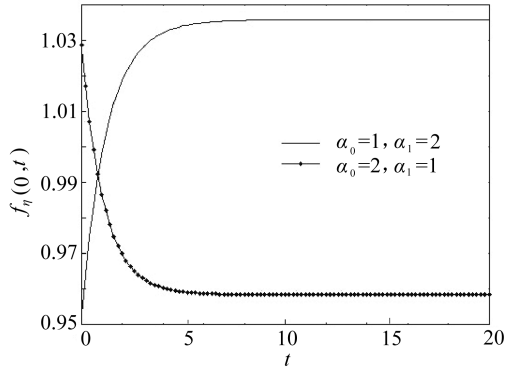
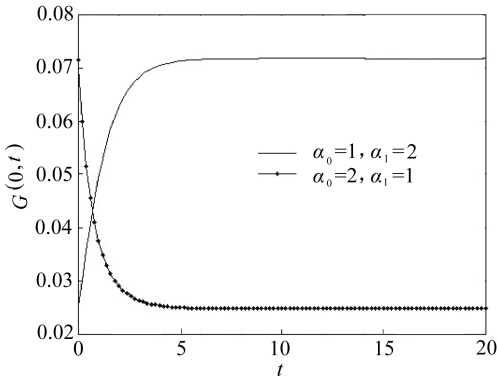


图 13 当  $Re_1 = 1, Re = -0.2, K = 0.5$  时,  $F_\eta(0, t), G(0, t)$  随时间的变化曲线

Fig. 13 The comparison of  $F_\eta(0, t), G(0, t)$  for different time as  $Re_1 = 1, Re = -0.2, K = 0.5$

## 5 结 论

本文对定常和非定常的膨胀率情况下的具有不同渗透的胀缩渗透管道中的流体流动进行了分析。定常的膨胀率情况下,原来的控制方程可以转化为常微分方程进行分析。而对应于非定常系数,则转化为偏微分方程。无论任何情况,都可以通过 HAM 方法得到其解析解。当膨胀率为常数时,不同的参数特别是壁面膨胀率对速度和微旋转速度的影响通过图形的方式进行了分析。当壁面的膨胀系数为时间函数时,可以得到一个重要的结论:即速度可以很快地接近稳态的状况,这说明时间的影响可以忽略不计。这样,控制方程则转化为常微分方程组。

对应非线性的常微分方程组,其非唯一解也许存在,并且受到参数  $A, K, Re, \alpha$  的影响。多解问题将是我们下一步的工作所在,有助于分析的进一步完善并且加深对于可变形壁面管道流动的理解。

**致谢** 本文作者衷心感谢评审人所提出的宝贵建议!

### 参考文献:

- [1] Berman A S. Laminar flow in channels with porous walls[J]. *Journal of Applied Physics*, 1953, **24**(9): 1232-1235.
- [2] Terrill R M, Thomas P W. Laminar flow in a uniformly porous pipe[J]. *Applied Science Research*, 1969, **21**(1): 37-67.
- [3] Terrill R M. On some exponentially small terms arising in flow through a porous pipe[J]. *The Quarterly Journal of Mechanics and Applied Mathematics*, 1973, **26**(3): 347-354.
- [4] Terrill R M. Laminar flow in a uniformly porous channel[J]. *The Aeronautical Quarterly*, 1964, **15**: 299-310.
- [5] Robinson W A. The existence of multiple solutions for the laminar flow in a uniformly porous channel with suction at both walls[J]. *Journal of Engineering Mathematics*, 1976, **10**(1): 23-40.
- [6] Terrill R M. Laminar flow through parallel and uniformly porous walls of different permeability[J]. *ZAMP*, 1965, **16**: 470-482.
- [7] Terrill R M, Shrestha G M. Laminar flow through parallel and uniformly porous walls of different permeability[J]. *Zeitschrift fur Angewandte Mathematik und Physik*, 1965, **16**: 470-482.
- [8] Uchida S, Aoki H. Unsteady flows in a semi-infinite contracting or expanding pipe[J]. *Journal of Fluid Mechanics*, 1977, **82**(2): 371-387.
- [9] Ohki Morimatsu. Unsteady flows in a porous, elastic, circular tube—part 1: the wall contracting or expanding in an axial direction[J]. *Bulletin of the JSME*, 1980, **23**(179): 679-686.
- [10] Goto M, Uchida S. Unsteady flow in a semi-infinite expanding pipe with injection through wall[J]. *Journal of the Japan Society for Aeronautical and Space Science*, 1990, **33**(9): 14-27.
- [11] Bujurke N M, Pai N P, Jayaraman G. Computer extended series solution for unsteady flow in a contracting or expanding pipe[J]. *IMA Journal of Applied Mathematics*, 1998, **60**(2): 151-165.

- [12] Majdalani J, Zhou C, Dawson C D. Two-dimensional viscous flow between slowly expanding or contracting walls with weak permeability [J]. *Journal of Biomechanics*, 2002, **35**(10): 1399-1403.
- [13] Dauenhauer C E, Majdalani J. Exact self-similarity solution of the Navier-Stokes equations for a porous channel with orthogonally moving walls[J]. *Physics of Fluids*, 2003, **15**(6): 1485-1495.
- [14] Majdalani J, Zhou C. Moderate-to-large injection and suction driven channel flows with expanding or contracting walls [J]. *Zeitschrift fur Angewandte Mathematik und Mechanik*, 2003, **83**(3): 181-196.
- [15] Asghar S, Mushtaq M, Hayat T. Flow in a slowly deforming channel with weak permeability: an analytical approach[J]. *Nonlinear Analysis:Real World Applications*, 2010, **11**(1): 555-561.
- [16] Si X H, Zheng L C, Zhang X X, Chao Y. Homotopy analysis solutions for the asymmetric laminar flow in a porous channel with expanding or contracting walls[J]. *Acta Mechanica Sinica*, 2011, **27**(2): 208-214.
- [17] Si X H, Zheng L C, Zhang X X, Chao Y. The flow of a micropolar fluid through a porous channel with expanding or contracting walls[J]. *Central European Journal of Physics*, 2011, **9**(3): 825-834.
- [18] 司新辉, 郑连存, 张欣欣, 晁莹. 半渗透涨缩管道内微极性流动解析求解[J]. *应用数学和力学*, 2010, **31**(9): 1027-1035. (SI Xin-hui, ZHENG Lian-cun, ZHANG Xin-xin, CHAO Ying. Analytic solution to the micropolar-fluid flow through a semi-porous channel with an expanding or contracting wall[J]. *Applied Mathematics and Mechanics(English Edition)*, 2010, **31**(9): 1073-1080.)
- [19] Xu H, Lin Z L, Liao S J, Wu J Z, Majdalani J. Homotopy based solutions of the Navier-Stokes equations for a porous channel with orthogonally moving walls[J]. *Physics of Fluids*, 2010, **22**(5): 053601.
- [20] Makukula Z G, Precious Sibanda Motsa S S. A novel numerical technique for two dimensional laminar flow between two moving porous walls[J]. *Mathematical Problems in Engineering*, 2010. ID 528956. doi:10.1155/2010/528956.
- [21] Si X H, Zheng L C, Zhang X X, Si X Y, Yang J H. flow of a viscoelastic through a porous channel with expanding or contracting walls [J]. *Chinese Physics Letters*, 2011, **28**(4): 044702.
- [22] Eringen A C. Theory of micropolar fluids[J]. *Journal of Mathematics & Mechanics*, 1966, **16**(1): 1-18.
- [23] Eringen A C. Theory of Thermomicropolar fluids[J]. *Journal of Mathematical Analysis and Applications*, 1972, **38**(2): 480-496.
- [24] Ariman T, Turk M A, Sylvester N D. Microcontinuum fluid mechanics—a review[J]. *International Journal of Engineering Science*, 1973, **11**(8): 905-930.
- [25] Ariman T, Turk M A, Sylvester N D. Application of Microcontinuum fluid mechanics—a review[J]. *International Journal of Engineering*, 1974, **12**(4): 273-293.
- [26] Eringen A C. *Microcontinuum Field Theories II ;Fluent Media* [M]. New York: Springer,

- 2001.
- [27] Subhadra Ramachandran P, Mathur M N, Ojha S K. Heat transfer in boundary layer flow of a micropolar fluid past a curved surface with suction and injection[J]. *International Journal of Engineering Science*, 1979, **17**(5): 625-639.
- [28] Takhar H S, Bhargava R, Agrawal R S, Balaji A V S. Finite element solution of micropolar fluid flow and heat transfer between two porous discs[J]. *International Journal of Engineering Science*, 2000, **38**(17): 1907-1922.
- [29] Kelson N A, Farrell T W. Micropolar fluid flow over a porous stretching sheet with strong suction or injection[J]. *International Communications in Heat and Mass Transfer*, 2001, **28**(4): 479-488.
- [30] Muhammad Ashraf, Anwar Kamal M, Syed K S. Numerical study of asymmetric laminar flow of a micropolar fluid in a porous channel[J]. *Computers & Fluids*, 2009, **38**(10): 1895-1902.
- [31] Muhammad Ashraf, Anwar Kamal M, Syed K S. Numerical simulation of flow of a micropolar fluid between a porous disk and a non-porous disk[J]. *Applied Mathematical Modelling*, 2009, **33**(4): 1933-1943.
- [32] Liao S J. *Beyond Perturbation: Introduction to Homotopy Analysis Method*[M]. Boca, Raton: Chapman Hall/CRC Press, 2003.
- [33] Liao S J. On the homotopy analysis method for nonlinear problems[J]. *Applied Mathematics and Computation*, 2004, **147**(2): 499-513.
- [34] Hayat T, Khan M. Homotopy solution for a generalized second grade fluid past a porous plate [J]. *Nonlinear Dynamics*, 2005, **42**(4): 395-405.
- [35] Hayat T, Khan M, Asghar S. Magnetohydrodynamic flow of an oldroyd 6-constant fluid[J]. *Applied Mathematics and Computation*, 2004, **155**(2): 417-225.
- [36] Hayat T, Khan M, Siddiqui A M, Asghar S. Transient flows of a second grade fluid[J]. *International Journal of Non-Linear Mechanics*, 2004, **39**(10): 1621-1633.
- [37] Abbas Z, Sajid M, Hayat T. MHD boundary-layer flow of an upper-convected Maxwell fluid in a porous channel[J]. *Theoretical and Computational Fluid Dynamics*, 2006, **20**(4): 229-238.
- [38] Sajid M, Hayat T, Asghar S. On the analytic solution of the steady flow of a fourth grade fluid [J]. *Physics Letters A*, 2006, **355**(1): 18-26.
- [39] Sajid M, Abbas Z, Hayat T. Homotopy analysis for boundary layer flow of a micropolar fluid through a porous channel[J]. *Applied Mathematical Modelling*, 2009, **33**(11): 4120-4125.
- [40] Srinivasacharya D, Ramana Murthy J V, Venugopalam D. Unsteady stokes flow of micropolar fluid between two parallel porous plates[J]. *International Journal of Engineering Science*, 2001, **39**(14): 1557-1563.
- [41] Rees D A S, Pop I. Free convection boundary layer flow of a micropolar fluid from a vertical flat plate[J]. *IMA Journal of Applied Mathematics*, 1998, **61**(2): 179-197.
- [42] Guram G S, Smith A C. Stagnation flows of micropolar fluids with strong and weak interactions[J]. *Computers & Mathematics With Applications*, 1980, **6**(2): 213-233.
- [43] Liao S J. An optimal homotopy-analysis approach for strongly nonlinear differential equations

[J]. *Communications in Nonlinear Science and Numerical Simulation*, 2010, **15**(8): 2003-2016.

## Homotopy Analysis Solution for Micropolar Fluid Flow Through Porous Channel With Expanding or Contracting Walls of Different Permeabilities

SI Xin-yi<sup>1</sup>, SI Xin-hui<sup>2</sup>, ZHENG Lian-cun<sup>2</sup>, ZHANG Xin-xin<sup>3</sup>

(1. *College of Water Conservancy and Hydropower Engineering, Hohai University, Nanjing 210098, P. R. China;*

2. *Department of Mathematics and Mechanics, University of Science and Technology Beijing, Beijing 100083, P. R. China;*

3. *Department of Mechanical Engineering, University of Science and Technology Beijing, Beijing 100083, P. R. China)*

**Abstract:** The flow of a micropolar fluid through a porous channel with expanding or contracting walls of different permeability was investigated. Two cases were considered in which the opposing walls undergo either uniform or nonuniform motion. In the first case, homotopy analysis method (HAM) was employed to obtain the expressions for velocity and micro-rotation fields. Graphs were sketched for some values of the parameters. The first conclusion can be made that expansion ratio and different permeability have important effects on the dynamic characteristics of the fluid. Following Xu's model, the second and more general case is that the wall expansion ratio varies with time. Under this assumption, the governing equations were transformed into nonlinear partial differential equations that also are solved analytically using HAM procedure. In the process, both algebraic and exponential models were considered to describe the evolution of  $\alpha(t)$  from the initial  $\alpha_0$  to a final state  $\alpha_1$ . As a result, it is found that the time-dependent solutions approach very rapidly to the steady state behavior. The second important conclusion can be made that the time-dependent variation of the wall expansion ratio plays a secondary role which may be justifiably ignored.

**Key words:** homotopy analysis method; micropolar fluid; expanding or contracting walls; porous channel; different permeability